Research Article
Academic Platform Journal of Natural Hazards and Disaster Management
4(2) 2023: 88-97, DOI: 10.52114/ apjhad.1398525

Effect of Different Scaling Methods on Seismic Isolator Behavior

Hakan Öztürk[1*], Gökhan Özdemir[2]

[1]Department of Civil Engineering, Faculty of Engineering, Sakarya University, Türkiye
[2]Department of Civil Engineering, ESQUAKE, Seismic Isolator Test Laboratory, Eskisehir Technical University, Türkiye

Received: / Accepted: 30-November-2023 / 25-December-2023

Abstract

This study investigated the maximum displacement, force, and acceleration values occurring at the isolation level in structures with lead rubber bearings using nonlinear response history analyses. Earthquake records used in the dynamic analysis were scaled with four different methods. In order to perform bi-directional analysis, both horizontal components of the earthquake records were applied to the isolation units simultaneously. In the analysis, the loss of strength (deterioration) due to the heating in the lead core due to the cyclical motion has been considered. In addition, in seismic isolated structures, five periods (Tiso=2.5s, 2.75s, 3.0s, 3.25s, and 3.5s) representing the isolation period, and four characteristic strength ratios (Q/W=0.75, 0.90, 0.105 and 0.120) representing the strength of the isolation unit were taken into account. As a result of the study, 10-13% change was observed in the maximum acceleration and displacement values at the isolation level due to different scaling methods. In addition, there was a 3% change in force results, and no significant difference occurred. Consequently, the isolation unit displacement and acceleration values differ significantly from earthquake to earthquake even though the scale coefficients derived from various scaling methods are relatively close to one another.

Key words: Lead rubber bearing, Scaling methods, Seismic isolation, OpenSees.

1. Introduction

The fundamental principle of seismic isolation application is to increase a structure period, thereby reducing potential earthquake loads and safeguarding structures from the destructive effects of earthquakes. The most significant parameters in the design of isolation units are the maximum isolation displacement (MID), maximum force transferred to the superstructure (MIF), and maximum acceleration (MA) values [1]. To determine these parameters, the nonlinear time history analysis method (NRHA) is recommended in codes [2–4]. The selection and scaling of earthquake records are crucial in this method [5]. Within the scope of selection of earthquake records, some criteria are defined in codes. However, apart from the criterion that the composite horizontal spectrum values of selected earthquake records should not be less than 1.3 times the design spectrum within the relevant period range, detailed information about scaling is lacking. Consequently, the method used for scaling is chosen by the design engineer.

* Corresponding author e-mail: hakanozturk@sakarya.edu.tr

Numerous studies in the literature have investigated various scaling methods concerning the scaling of earthquake records [6–14]. Kalkan and Chopra developed the modal pushover-based scaling method, abbreviated as MPS, and compared it with methods provided in ASCE/SEI 7-05 [15]. Similarly, Huang et al. compared the D-scaling method proposed by them with existing methods in the literature [16]. Pant and Maharjan examined isolator displacement using different scaling methods in seismic isolated structures [17]. Michaud and Leger investigated nine different scaling methods for fixed base structures and compared the resulting structural responses [18]. Pant utilized amplitude scaling and spectral matching methods to determine structural responses in buildings with seismic isolators [19].

In the studies carried out in the literature within the scope of scaling of earthquake records, fixed base structures are generally considered. However, few studies have been conducted for seismically isolated structures, neglecting strength loss due to lead core heating. In this study, the effects of different scaling methods on the behavior of isolating units, considering the maximum isolation displacement (MID), maximum force (MIF), and maximum acceleration (MA) values, were examined by taking into account the strength loss caused by temperature increase due to cyclic behavior in lead rubber bearings (LRBs). Earthquake records selected for dynamic analysis were scaled using four different methods, and all records were simultaneously applied to the isolating unit model for bi-directional analyses. Furthermore, to determine the structural responses (MID, MIF, and MA) in the isolating unit, isolation period (Tiso) and characteristic strength ratio (Q/W) values were selected as parameters. Thus, five periods representing isolation period (Tiso=2.5s, 2.75s, 3.0s, 3.25s, and 3.5s), and four characteristic strength ratios representing strength (Q/W=0.75, 0.90, 0.105, and 0.120) were considered in the analyses.

2. Modeling of LRB

The isolation unit investigated in this study was modeled as a single-degree-of-freedom system. The OpenSees [20] structural analysis program was utilized for seismic isolation unit analyses. A superstructure weight of 1308 kN was determined and applied to the isolation unit. A representative visualization of the LRB used in the study is presented in Figure 1a. The strength loss due to the temperature rise in the lead core occurs gradually in each cycle [21-23]. This behavior, illustrated in Figure 1b, is derived from test results conducted on LRB. In the analyses, the shear stress of the lead core (σYL0) was chosen as 10 MPa, and the shear stress of the rubber (G) was set to 0.5 MPa.

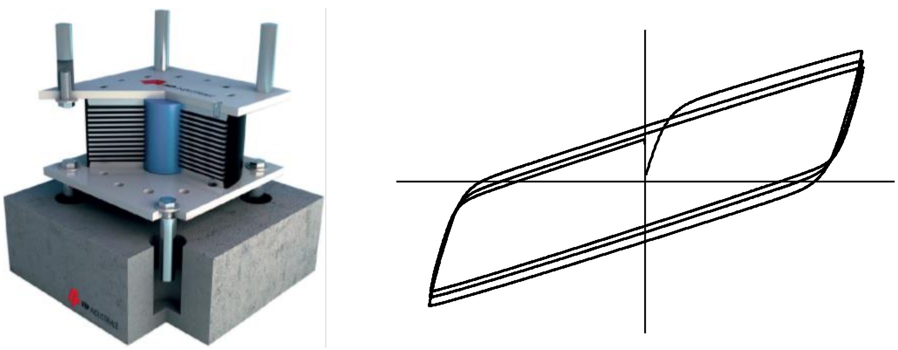

a) b)

Figure 1. a) Lead rubber bearing [24] and b) force-displacement behavior [25]

3. Selection and Scaling of Earthquake Records

The criteria defined in the codes were considered in the selection of earthquake records for the study. These criteria consist of magnitude (Mw) between 6.5 and 7.6, distance from fault rupture (R) less than 20 km, and shear wave velocity (Vs) in the top 30m of the soil ranging from 180m/s to 360m/s. The earthquake records listed in Table 1, with their characteristics detailed, were obtained from the Pacific Earthquake Engineering Research Center (PEER) database [26]. The PGA, PGV, and PGD presented in Table 1 represent the peak ground acceleration, velocity, and displacement.

Table 1. Information about earthquake records

EQ Number	EQ Name	Station	Magnitude (M_w)	R (km)	Component	PGA (g)	PGV (cm/s)	PGD (cm)
1	Kocaeli	Duzce	7,5	15,4	180	0,31	58,9	44,2
					270	0,36	46,4	17,6
2	Kocaeli	Yarimca	7,5	4,8	060	0,27	65,7	57,2
					330	0,35	62,2	51,1
3	Erzincan	Erzincan	6,7	4,4	NS	0,52	84,0	27,7
					EW	0,50	64,3	21,9
4	Imperial Valley	El Centro Array #4	6,5	7,1	230	0,36	76,5	58,9
					140	0,49	37,4	19,7
5	Imperial Valley	El Centro Array #5	6,5	4,0	230	0,38	90,5	63,0
					140	0,52	46,9	35,3
6	Duzce	Duzce	7,1	6,6	270	0,54	83,5	51,8
					180	0,35	60,0	41,8
7	Imperial Valley	El Centro Array #10	6,5	6,2	050	0,17	47,5	31,1
					320	0,22	41,2	18,0
8	Chi-Chi	CHY024	7,6	9,6	W	0,28	52,9	43,6
					N	0,18	49,0	31,1
9	Duzce	Bolu	7,1	12,0	090	0,82	62,1	13,6
					000	0,73	56,4	23,1
10	Chi-Chi	TCU109	7,6	13,1	N	0,16	53,1	34,8
					W	0,16	50,8	46,5
11	Kobe	KJM	6,9	1,0	000	0,82	81,3	17,7
					090	0,60	74,4	20,0

This study adopted the simple scaling method recommended by codes as a reference and investigated the extent to which four different scaling methods affected the responses in the isolation unit. Scaling considered earthquake ground motion levels with exceedance probabilities of 2% (DD-1) and 10% (DD-2) over 50 years. For these ground motion levels, the 1s design spectral acceleration values (SD1) were determined as 0.87 and 0.56, respectively. Each earthquake record was separately scaled for the five isolation periods considered in the study [27].

The scale factors obtained through the examined scaling methods for each earthquake and each period value are provided in Table 2. Additionally, the compatibility of the spectrum curves generated using these methods with the DD-1 (MCE) and DD-2 (DBE) spectrum curves is presented in Figure 2a and Figure 2b, respectively.

Table 2. Scale Factors

Period	Scaling Method	EQ1	EQ2	EQ3	EQ4	EQ5	EQ6	EQ7	EQ8	EQ9	EQ10	EQ11	Average
T=2,5 s	M1						1,38						
	M2	1,40	1,26	1,03	1,48	1,21	1,33	1,88	1,83	1,80	1,30	1,19	1.43
	M3	1,64	1,32	0,86	1,30	1,53	1,08	1,44	1,92	1,69	1,84	1,30	1.35
	M4	1,44	1,22	1,02	1,57	1,22	1,30	1,88	1,73	1,68	1,23	1,30	1.42
T=2,75 s	M1						1,38						
	M2	1,40	1,26	1,03	1,48	1,21	1,33	1,88	1,83	1,80	1,30	1,19	1.43
	M3	1,64	1,32	0,93	1,30	1,52	1,08	1,35	1,73	1,68	1,68	1,40	1.42
	M4	1,44	1,22	1,02	1,57	1,22	1,30	1,88	1,73	1,68	1,23	1,30	1.42
T=3,0 s	M1						1,38						
	M2	1,38	1,24	1,02	1,46	1,20	1,32	1,85	1,81	1,77	1,29	1,17	1.43
	M3	1,56	1,26	1,00	1,22	1,40	1,03	1,29	1,51	2,13	1,40	1,57	1.40
	M4	1,44	1,22	1,02	1,57	1,22	1,30	1,88	1,73	1,68	1,23	1,30	1.42
T=3,25 s	M1						1,36						
	M2	1,37	1,23	1,01	1,45	1,18	1,31	1,84	1,79	1,76	1,27	1,17	1.40
	M3	1,54	1,24	1,18	1,05	1,26	1,02	1,34	1,40	2,26	1,08	1,69	1.37
	M4	1,41	1,20	1,00	1,54	1,20	1,28	1,84	1,69	1,65	1,21	1,27	1.39
T=3,5 s	M1						1,33						
	M2	1,34	1,20	0,99	1,42	1,16	1,28	1,80	1,76	1,73	1,25	1,14	1.37
	M3	1,49	1,20	1,30	0,96	1,12	0,98	1,37	1,35	2,18	1,00	1,82	1.34
	M4	1,38	1,17	0,99	1,51	1,18	1,25	1,81	1,66	1,62	1,19	1,25	1.36

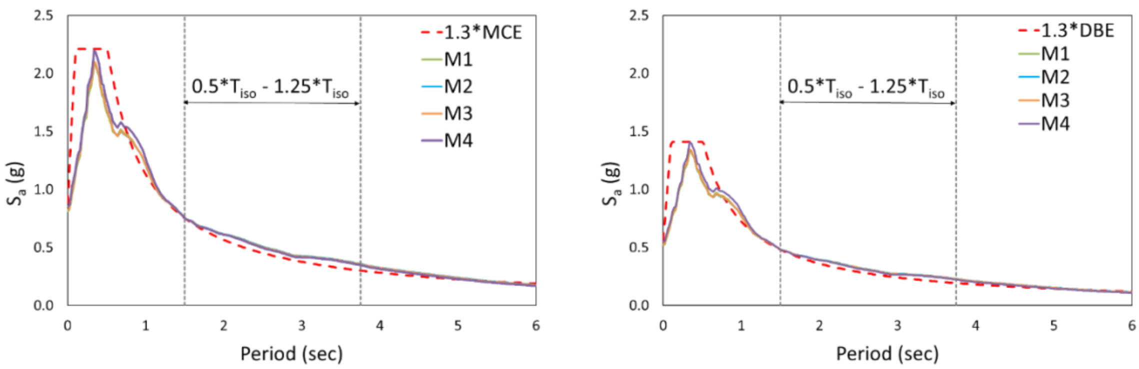

a) b)

Figure 2. a) DD-1 (MCE) spectrum and scaling methods for T=3.0 (sec) b) DD-2 (DBE) spectrum and scaling methods for T=3.0 (sec)

4. Analysis Results

Results of DD-1 earthquake ground motion levels were considered for MID values obtained from dynamic analyses, while DD-2 earthquake ground motion levels were considered for MIF and MA. In determining isolation unit displacement and acceleration values, the square root of the sum of squares ($\sqrt{x^2+y^2}$) rule was applied to data obtained from both directions. The maximum force value was determined as the greater of the values obtained from both directions. The results of the study are presented below as the isolation period effect (Figures 3-5) and the characteristic strength ratio effect (Figures 6-8). In the graphs presented, the vertical axis shows MID, MIF, and MA, respectively, while the horizontal axis represents the scaling methods used in the study. The numerical values given show the largest, average, and smallest values of the results of 11 earthquake records for each scaling method.

4.1. Effect of isolation period

This section examines the variation of MID, MIF, and MA values based on the isolation period. For this purpose, the characteristic strength ratio was kept constant (Q/W=0.105). The MID, MIF, and MA results obtained from the analyses are presented in Figures 3-5, respectively. When Figure 3 is examined, differences between 3% and 10% were obtained when the MID obtained for each period was compared with the M1 scaling method chosen as reference and other scaling methods used. It is seen that this change increases with the increase in period. For constant Q/W (0.105), the MID value obtained from each scaling method varies for different period values. For example, the largest MID values for the 2.5s and 2.75s periods were obtained from the M4 method, while the largest MID values for the 3.0s, 3.25s, and 3.5s periods were obtained from the M1 method. Values ranging between 6.3% and 9.5% were found between the largest and smallest values in the MID obtained from the scaling methods at each period value (9.2, 8.6, 6.3, 7.7, 9.5%). Among the scaling methods, the most scatter occurred in the M1 and M4 methods, while the least scatter occurred in the M2 method.

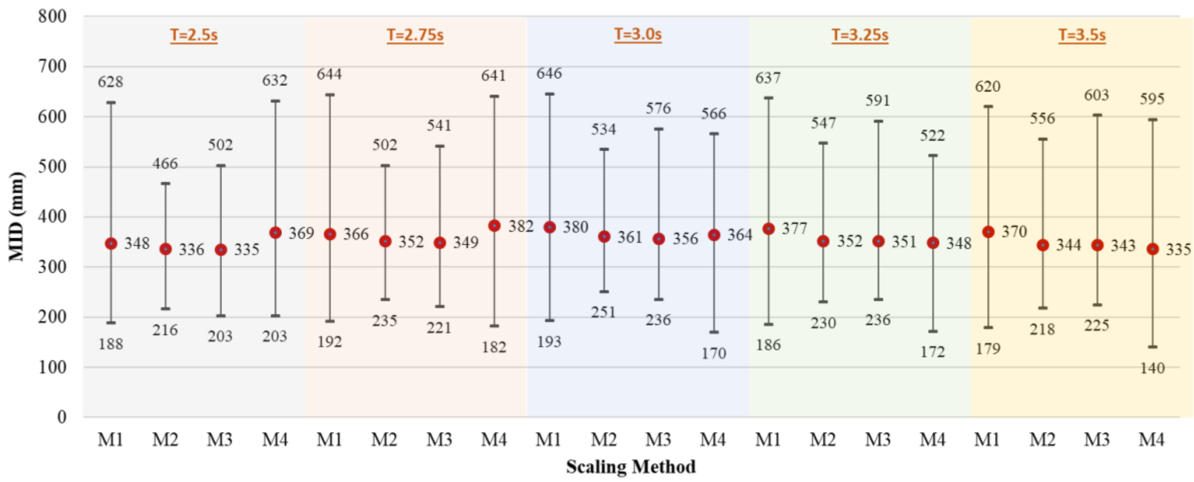

Figure 3. Variation of MID with period and scaling methods (Q/W=0.105)

The variation of MIF values concerning the isolation period and scaling methods is presented in Figure 4. When comparing MIF values obtained for each period using different scaling methods, closely similar results are observed. In comparison to the selected M1 scaling method, the difference in MIF results obtained from other scaling methods is mostly around 3%. The most significant MIF values are derived from the M1 scaling method, while the smallest originate from the M4 scaling method. It is evident that, under a fixed Q/W ratio (0.105), the MIF values decrease with an increase in the period. However, the MIF variation among scaling methods for each isolation period is quite small and could be considered negligible.

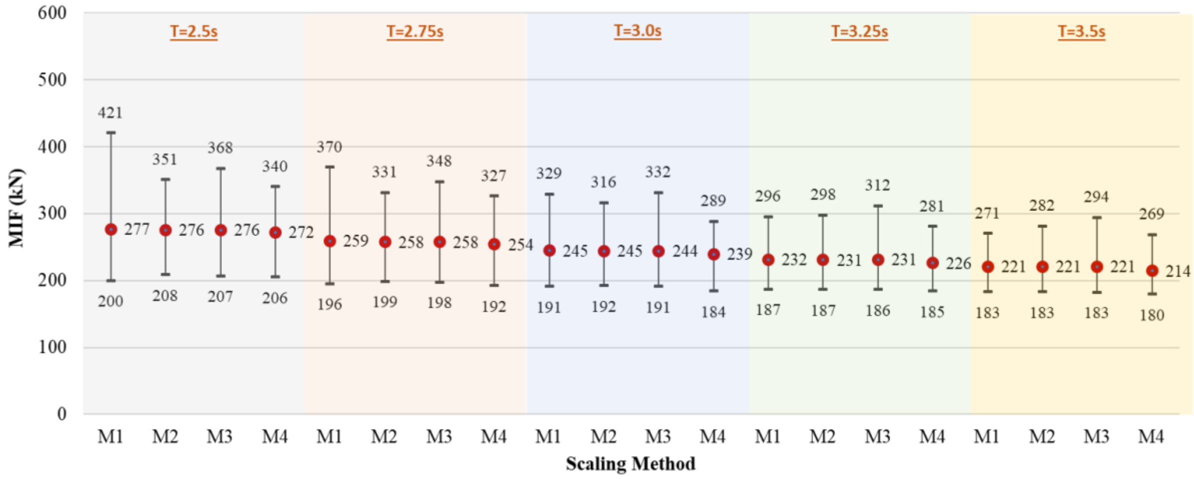

Figure 4. Variation of MIF with period and scaling methods (Q/W=0.105)

Figure 5 presents the changes in MA values depending on the isolation period and scaling methods. Different results were obtained when the MA obtained for each period value was compared using different scaling methods. Compared to the M1 scaling method chosen as a reference, MA results from other scaling methods vary between 6.2% and 12.8%. The most significant MA values were obtained from the M2 scaling method, and the smallest MA values were obtained from the M1 scaling method. For a fixed Q/W ratio (0.105), MA values decrease with the increase of the period.

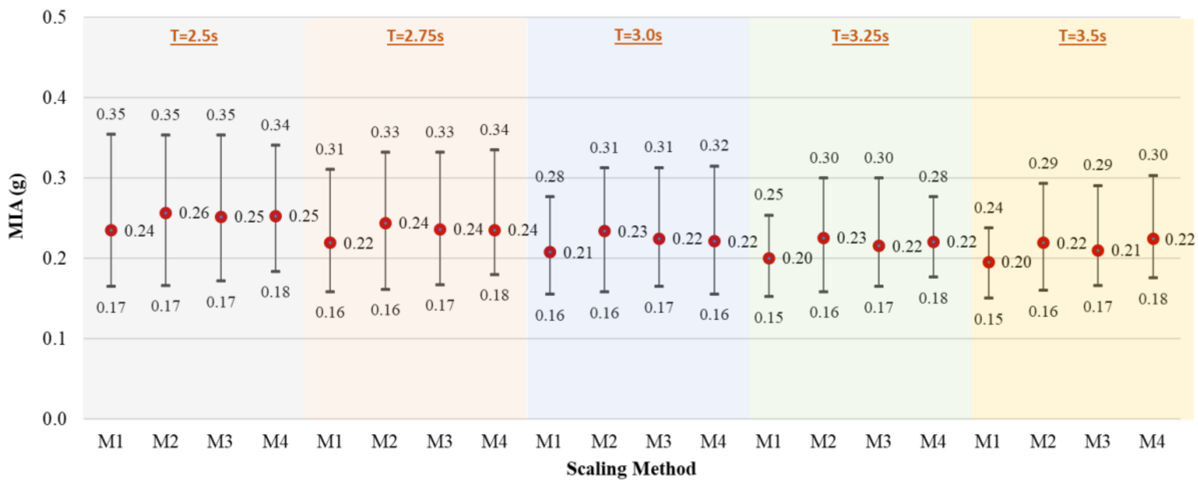

Figure 5. Variation in MA based on period and scaling methods (Q/W=0.105)

4.2. Effect of characteristic strength ratio

This section examined the variation of MID, MIF, and MA values with respect to the characteristic strength ratios. For this purpose, the isolation period (T_{iso}=3.0s) was kept constant. The MID, MIF, and MA results obtained from the analysis are presented in Figures 6-8, respectively. Figure 6 illustrates differences ranging from 2.7% to 6.9% in MID obtained for each characteristic strength ratio compared to other scaling methods using the selected reference method, M1. As the characteristic strength ratio increases, MID decreases. For the fixed isolation period (3.0s), the MID values obtained from each scaling method vary for different characteristic strength ratio values. While the largest MID values are derived from the M1 method, the smallest MID values are obtained from the M3 method. Only for the characteristic strength ratio of 0.120, the smallest MID value occurs in the M4 method. Among the MID values obtained from scaling methods for each characteristic strength ratio, there are variations between the largest and smallest values ranging from 4.5% to 6.3% (5.3, 6.3, 6.3, 4.5). The maximum scattering is observed among the M1 and M4 methods, while the minimum scattering appears with the M2 method.

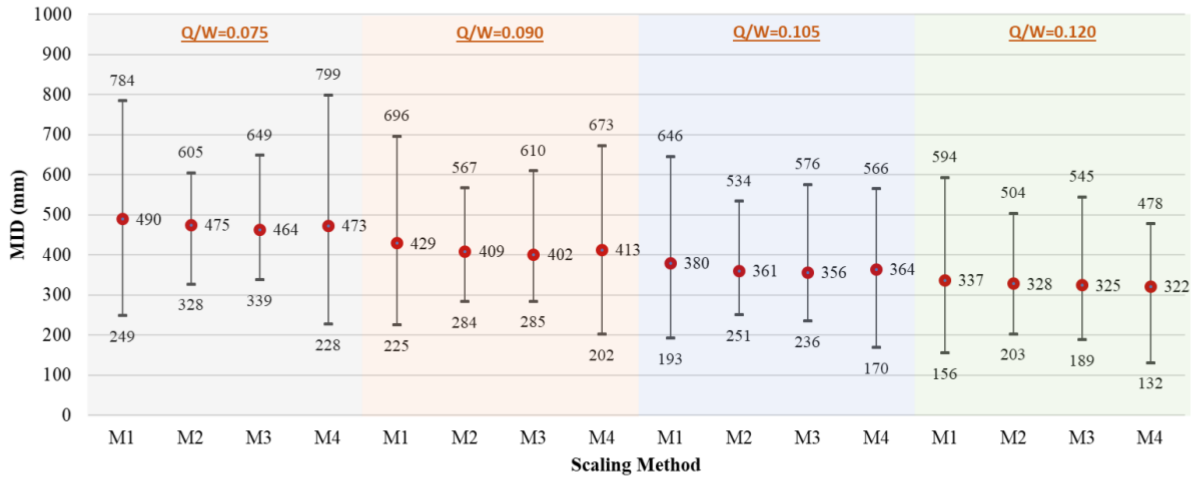

Figure 6. Variation of MID with respect to characteristic strength and scaling methods (T=3.0 sec.)

The change of MIF values depending on the characteristic strength ratio and scaling methods is presented in Figure 7. When the MIF values for each characteristic strength ratio were compared using different scaling methods, very similar results were obtained. Compared to the M1 scaling method chosen as a reference, MIF results from other scaling methods vary between 0.16% and 2.54%. It is seen that MIF values increase due to the increase in the characteristic strength ratio for the fixed isolation period (3.0s). However, the change between scaling methods for each characteristic strength ratio is quite small and negligible.

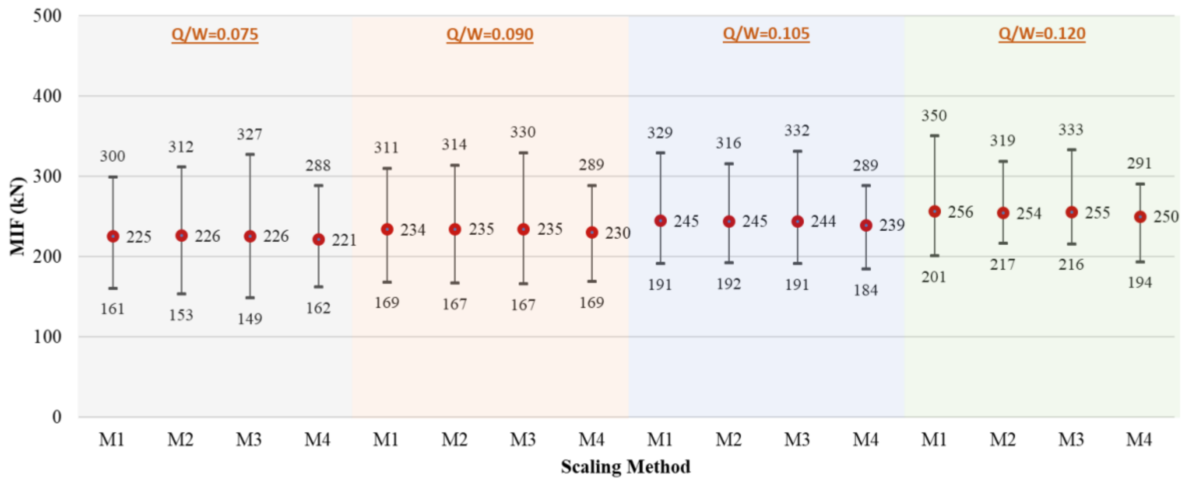

Figure 7. Displays the alteration in MIF concerning characteristic strength and scaling methods at T=3.0 sec.

The change of MA values depending on the characteristic strength ratio and scaling methods is presented in Figure 8. Different results were obtained when the MA obtained for each characteristic strength ratio was compared using different scaling methods. Compared to the M1 scaling method chosen as a reference, MA results from other scaling methods vary between 5.1% and 11.2%. It is seen that MA values increase due to the increase in the characteristic strength ratio for the fixed isolation period (3.0s).

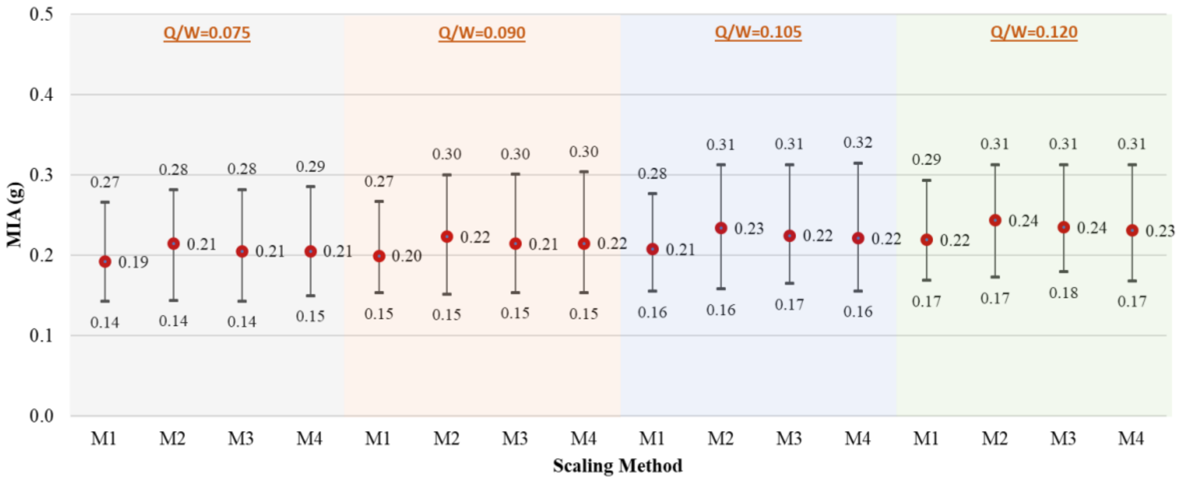

Figure 8. Variation of MA according to characteristic strength and scaling methods (T=3.0 sec.)

5. Conclusions and Results

In this study, lead-rubber bearings were examined considering strength degradation, focusing on the maximum displacement (MID), force (MIF), and acceleration (MA) values using different scaling methods. Scaled earthquake records were simultaneously applied to the isolation system for bi-directional analyses. Structural responses (MID, MIF, and MA) were determined for five different isolation periods (T_{iso}=2.5s, 2.75s, 3.0s, 3.25s, and 3.5s) and four characteristic strength ratios (Q/W=0.75, 0.90, 0.105, and 0.120) selected as parameters for comparison. The findings from the analysis are provided below.

- As a result of different scaling methods, different scale coefficients were obtained for each earthquake.
- While displacements increase in parallel with the increase in the isolation period, displacements decrease due to the increase in the characteristic strength ratio.
- When the force data is examined, it decreases in parallel with the increase in the isolation period, while it increases depending on the increase in the characteristic strength ratio.
- While acceleration values decrease in parallel with the increase in the isolation period, they increase depending on the increase in the characteristic strength ratio.

As a result, although the scale coefficients obtained from different scaling methods are close to each other for each earthquake, there are significant differences in the isolation unit displacement and acceleration values. This variation is negligible for the force data obtained in the study.

Acknowledgment

This study was funded by the project number 118C510 within the scope of the 2218 program of the Turkish Scientific and Technical Research Council (TUBITAK).

This study was presented at the 10th International Symposium on Innovative Technologies in Engineering and Science, ISITES2022.

Conflict of Interests

The authors declare that they have no known competing financial interests or personal relationships that could have appeared to influence the work reported in this paper.

Author Contributions

Hakan Öztürk and Gökhan Özdemir contributed to the design and implementation of the research to the analysis of the results and to the writing of the manuscript.

References

[1] Naeim, F., and Kelly, J. M. (1999). Design of seismic isolated structures : from theory to practice. John Wiley.

[2] Turkish Building Earthquake Code (TBEC), Principles for the design of buildings under earthquake, Ankara, Turkey, 2018.

[3] Eurocode8: Design of Structures for Earthquake Resistance- Part 1: General Rules, Seismic Actions and Rules for Buildings, EN 1998-1, 2004.

[4] American Society of Civil Engineers/Structural Engineering Institute, 2016. Minimum Design Loads For Buildings And Other Structures, ASCE/SEI 7-16, Reston, V.A.

[5] Bommer JJ, Acevedo AB. The use of real earthquake accelerograms as input to dynamic analysis. *J Earthq Eng* 2004;8:43–91.

[6] Nau JM, Hall WJ. Scaling Methods for Earthquake Response Spectra. *J Struct Eng* 1984;110:1533–48.

[7] Shome N, Cornell CA, Bazzurro P, Carballo JE. Earthquakes, records, and nonlinear responses. *Earthq Spectra* 1998;14:469–500.

[8] Malhotra PK. Strong-motion records for site-specific analysis. *Earthq Spectra* 2003;19:557–78.

[9] Weng Y.T., Tsai K.C., Chan Y.R. A ground motion scaling method considering highermode effects and structural characteristics. *Earthq Spectra* 2010;26:841–786.

[10] Kwong NS, Chopra AK, Mcguire RK. A framework for the evaluation of ground motion selection and modification procedures. *Earthq Eng Struct Dyn* 2015;44:795–815.

[11] Marasco S, Cimellaro GP. A new energy-based ground motion selection and modification method limiting the dynamic response dispersion and preserving the median demand. *Bull Earthq Eng* 2018;16:561–81.

[12] Kottke A, Rathje EM. A Semi-Automated Procedure for Selecting and Scaling Recorded Earthquake Motions for Dynamic Analysis. Earthq Spectra 2019;24:911–32.

[13] Zhang R, Wang D, Chen X, Li H. Weighted and Unweighted Scaling Methods for Ground Motion Selection in Time-history Analysis of Structures. *J Earthq Eng* 2020:1–36.

[14] Eren N, Sucuoğlu H, Pinho R. Interstory drift based scaling of earthquake ground motions. *Earthq Eng Struct Dyn* 2021;50:3814–30.

[15] Kalkan E, Chopra AK. Modal-Pushover-Based Ground-Motion Scaling Procedure. *J Struct Eng* 2011;137:298–310.

[16] Huang Y-N, Whittaker AS, Luco N, Hamburger RO. Scaling Earthquake Ground Motions for Performance-Based Assessment of Buildings. *J Struct Eng* 2011;137:311–21.

[17] Pant DR, Maharjan M. On selection and scaling of ground motions for analysis of seismically isolated structures. *Earthq Eng Eng Vib* 2016;15:633–48.

[18] Michaud D, Léger P. Ground motions selection and scaling for nonlinear dynamic

analysis of structures located in Eastern North America. *Can J Civ Eng* 2014;41:232–44.

[19] Pant DR. Influence of scaling of different types of ground motions on analysis of code-compliant four-story reinforced concrete buildings isolated with elastomeric bearings. *Eng Struct* 2017;135:53–67.

[20] Open System for Earthquake Engineering Simulation (OpenSees), 2021. Version: 3.3.0, Software, University of California, Pacific Earthquake Engineering Research Center, Berkeley, California, 2021. http://opensees.berkeley.edu.

[21] Alhan C, Şahin F. Protecting vibration-sensitive contents: An investigation of floor accelerations in seismically isolated buildings. *Bull Earthq Eng* 2011;9:1203–26.

[22] Robinson WH. Lead-Rubber Hysteretic Bearings Suitable for Protecting Structures During Earthquakes. *Earthq Eng Struct Dyn* 1982;10:593–604.

[23] Ozdemir G, Dicleli M. Effect of lead core heating on the seismic performance of bridges isolated with LRB in near-fault zones. *Earthq Eng Struct Dyn* 2012;41:1989–2007.

[24] Charleson, A.; Guisasola, A. Seismic Isolation for Architects; Routledge: London, UK; New York, NY, USA, 2017.

[25] Ozdemir G, Constantinou MC. Evaluation of equivalent lateral force procedure in estimating seismic isolator displacements. Soil Dyn Earthq Eng 2010;30:1036–42.

[26] PEER Ground Motion Database-Beta Version With special thanks to: Technical Report for the PEER Ground Motion Database Web Application. 2010.

[27] Öztürk, H. Effects of Lead Core Heating on the Response of Isolated-Base and Fixed-Base Regular and Irregular Reinforced Concrete Structures. *Buildings* 2022, 12, 1087. https://doi.org/10.3390/buildings12081087